# STRUCTURE CHARACTERIZATION AND NONLINEAR OPTICAL PROPERTIES OF NOVEL CHALCONE DERIVATIVES: EXPERIMENTAL AND COMPUTATIONAL INVESTIGATIONS

**FARAH DIANA BINTI RAMZI**

**UNIVERSITI SAINS MALAYSIA**

**2024**

# STRUCTURE CHARACTERIZATION AND NONLINEAR OPTICAL PROPERTIES OF NOVEL CHALCONE DERIVATIVES: EXPERIMENTAL AND COMPUTATIONAL INVESTIGATIONS

**by**

**FARAH DIANA BINTI RAMZI**

**Thesis submitted in fulfilment of the requirements**
**for the degree of**
**Master of Science**

**November 2024**

## ACKNOWLEDGEMENT

I am deeply grateful to Allah SWT for giving me the strength and blessing to complete this master's thesis successfully.

First and foremost, I would like to express my sincere appreciation to my supervisor, Assoc. Prof. Dr. Quah Ching Kheng, for his invaluable mentorship and dedication throughout this journey. His patience and enthusiasm were invaluable, and his encouragement and useful critiques helped me to improve my research throughout the process. I am truly grateful for his guidance and support.

I would like to dedicate this dissertation to my beloved parents, Mr. Ramzi and Mrs. Musliza, for all the prayers and sacrifices they have made to make me a successful and better person. Your love and support have been my guiding light throughout my journey. Thank you for always believing in me, even when I didn't believe in myself. To all my dearest siblings, a big thank you for their support, inspiration and for putting colors in my life. May Allah always bless you all. Also, I would like to dedicate my appreciation to my husband, Mr. Muhammad Azri for your endless support and motivation to complete this thesis. Thank you for being a part of my journey and persuading me to never give up on this challenging journey.

My deepest thanks go to my fellow lab mate, Ms. Wong Qin Ai for her never-ending support and assistance in my research project. She has always been willing to teach, help, and give me her ideas, and I am truly grateful for her friendship and mentorship. I would also like to thank the staff of the X-ray Crystallography laboratory, especially Mr. Aswafi, Mr. Mustaqim Rosli and Mr. Mustaqim Abu Bakar for their support and assistance in conducting my research project. I am grateful for their willingness to help me whenever I needed it. I am also grateful to my other lab

mates and friends, Ms. Aliya, Ms. Farhana, Mr. Amin, Ms. Aisyah, Mr. Ooi, Mr. Saleh and Mr. Aizat for their support and encouragement. They have always been there for me, both academically and personally, and I am so grateful for their friendship. Not forgetting, I would also like to express my appreciation to Dr. Dian Alwani and Dr. Suhana for their encouragement and insightful comments. Their feedback helped me to improve my thesis.

I am also grateful to the Malaysian government and the Universiti Sains Malaysia for their financial support for this work through the Fundamental Research Grant Scheme (203.PFIZIK.6711899).

Finally, I would like to thank everyone who has been a part of my life directly or indirectly during my master's journey. I am truly grateful for your support and encouragement.

## TABLE OF CONTENTS

## LIST OF TABLES

**Page**

## LIST OF FIGURES

**Page**

## LIST OF SYMBOLS

| | |
|---|---|
| $C$ | Curvedness |
| $E_{dis}$ | Grimme's D2 dispersion correction |
| $E_{ele}$ | Classical electrostatic interaction energy between charge distributions of monomers |
| $E_{ex}$ | Excitation energy |
| $E_{pol}$ | Polarization energy |
| $J$ | Coupling constant |
| $P_L$ | Linear optic |
| $P_{NL}$ | Nonlinear optic |
| $S$ | Shape index |
| $T_{min}$, $T_{max}$ | Minimum and maximum transmission factors applied to the diffraction pattern |
| $U_{iso}$, $U_{eq}$ | Isotropic atomic displacement parameter, equivalent isotropic atomic displacement parameter |
| Z | Asymmetric unit |
| $\alpha$ | Optical absorption coefficient |
| α | Polarizability |
| $\alpha_2$ | Nonlinear absorption coefficient |
| β | First hyperpolarizability |
| β | Interaxial angle between a and c-axis |
| $d_e$ / $d_i$ | Distances between a specific point on the Hirshfeld surface and the external/internal surfaces of the nearest |
| $\varepsilon_i$ | Wavefunction of the $i^{th}$ electron |
| $\varepsilon_0$ | Permittivity of free space |
| $f_0$ | Oscillator strength |
| $h$ | Planck constant |
| $n_2$ | Nonlinear refractive index coefficient |
| δ | Delta |

| | |
|---|---|
| μ | Dipole moment |
| $v$ | Frequency of the incident photons |
| ν | Stretching |
| λ | Wavelength |
| γ | Out of plane bending |
| γ | Second hyperpolarizability |
| χ | Susceptibility of the medium |
| Δr | Descriptor on the metric of charge transfer molecular excitations |
| $\rho_0(r)$ | Electron density |
| $\phi_i(r)$ | Energy of the electron in the $i^{th}$ orbital |
| $\left(\frac{dn}{dT}\right)$ | Thermal-optical coefficient |
| ⟨i\|μ\|j⟩ | Variation of dipole moment |

## LIST OF ABBREVIATIONS

| | |
|---|---|
| 2PA | Two-Photon Absorption |
| A | Acceptor |
| ATR | Attenuated Total Reflection |
| B3LYP | Becke's 3-Parameter (Exchange) and Lee-Yang-Parr (Correlation) |
| CAM-B3LYP | Coulomb-Attenuating Method B3lyp |
| CCD | Charge-Coupled Device |
| CCDC | Cambridge Crystallographic Data Centre |
| CW | Continuous Wave |
| D | Donor |
| DC-Kerr | Electro-Optic Kerr Effect |
| DFT | Density Functional Theory |
| DMF | N, N-Dimethylformamide |
| EFISHG | Electric-Field Induced Optical Second Harmonic Generation |
| EOPE | Electro-Optic Pockels Effect |
| EXP | Experiment |
| FMOs | Frontier Molecular Orbitals |
| FOMs | Figure Of Merits |
| FP | Fingerprint Plot |
| FTIR | Fourier Transform Infrared |
| FWM | Four-Wave Mixing |
| GGA | Generalized Gradient Approximation |
| GIAO | Gauge-Independent Atomic Orbital |
| GTO | Gaussian Type Orbitals |
| HOMO | Highest Occupied Molecular Orbital |
| ICT | Intramolecular Charge Transfer |
| IDRI | Intensity-Dependent Refractive Index |
| IEFPCM | Integral Equation Formalism Variant Polarizable Continuum Model |
| IR | Infrared |
| LUMO | Lowest Unoccupied Molecular Orbital |
| MEP | Molecular Electrostatic Potential |
| NLA | Nonlinear Absorption |

| | |
|---|---|
| NLO | Nonlinear Optics |
| NLR | Nonlinear Refraction |
| NMR | Nuclear Magnetic Resonance |
| NPA | Natural Population Analysis |
| OA/CA | Open / Close Aperture |
| OL | Optical Limiting |
| ORTEP | Oak Ridge Thermal Ellipsoid Plot |
| PCM | Polarizable Continuum Model |
| PPM | Parts Per Million |
| RMSD | Root-Mean-Square Deviation |
| SADABS | Siemens Area Detector Absorption Correction |
| SAINT | SAX Area-Detector Integration (SAX-Siemens Analytical Xray) |
| SCF | Self-Consistent Field |
| SCXRD | Single Crystal X-Ray Diffraction |
| sEDA/ pEDA | $\sigma$ and $\pi$ -Electron Donor-Acceptor |
| SHG | Second Harmonic Generation |
| SMART | Siemens Molecular Analysis Research Tools |
| SPM/XPM | Self/Cross Phase Modulation |
| STOs | Slater-Type Orbitals |
| TDDFT | Time-Dependent Density Functional Theory |
| THG | Third-Harmonic Generation |
| TMS | Tetramethylsilane |
| UV-Vis | Ultraviolet Visible |
| USM | Universiti Sains Malaysia |
| vdW | van der Waals |

## LIST OF APPENDICES

**PENCIRIAN STRUKTUR DAN SIFAT OPTIK TAKLINEAR TERHADAP SEBATIAN KALKON BAHARU: KAJIAN EKSPERIMEN DAN KOMPUTASI**

## ABSTRAK

Lapan sebatian kalkon fluoro metoksi fenil (**1**-**8**) dengan kumpulan substituen yang berbeza telah disintesis dengan menggunakan kaedah pemeluwapan Claisen-Schmidt dan dihablurkan menggunakan teknik penyejatan secara perlahan. Sebatian telah dicirikan menggunakan FTIR dan NMR manakala, struktur 3D telah disahkan menggunakan SCXRD. Analisis permukaan Hirshfeld mendedahkan bahawa pembungkusan hablur dan konformasi molekul telah distabilkan melalui ikatan hidrogen, penyusunan π–π, dan interaksi halogen. Sifat molekul telah ditentukan menggunakan analisis MEP dan NPA. Sifat optik linear dan taklinear tertib ketiga telah dikaji secara teori (menggunakan DFT dan TDDFT) dan secara eksperimen (menggunakan spektrometer UV-VIS dan teknik imbasan Z-scan). Kajian teori menunjukkan bahawa kemuncak penyerapan sebatian **1**-**8** sebahagian besarnya disumbangkan oleh peralihan elektronik dari keadaan dasar kepada keadaan teruja kedua ($S_0 \rightarrow S_2$) dengan tenaga pengujaan antara 4.17 hingga 4.29 eV, dan momen dipol elektronik peralihan antara 2.763 hingga 2.885 a.u. Kajian eksperimen menentukan penyerapan dua foton (2PA) dalam kesemua sebatian adalah disebabkan oleh penyerapan taklinear (NLA) dalam rejim laser bukan resonan, selaras dengan aliran $\gamma_{DFT}$ dinamik (-ω;ω,ω,-ω) yang dikira menggunakan fungsi CAM-B3LYP pada panjang gelombang 637 nm. Selain itu, penerangan bagi metrik pemindahan cas pengujaan molekul, Δr, berkolerasi baik dengan penyerapan taklinear $\alpha_2$ yang diperoleh melalui eksperimen imbasan-Z apertur terbuka, dan hiperpolarisabiliti

peringkat kedua yang dikira menggunakan DFT. Pembiasan taklinear (NLR) yang diperhatikan melalui eksperimen imbasan-Z apertur tertutup menunjukkan bahawa nilai negatif NLR adalah disebabkan oleh tingkah laku pemfokusan kendiri kesemua sebatian. Aliran $n_2$ untuk kesemua sebatian yang sama dengan aliran eksperimen $\gamma_{exp}$ (-ω;ω,ω,-ω) menunjukkan bahawa NLR mungkin dipengaruhi secara langsung oleh difusiviti termal yang berbeza setiap sebatian dengan pengganti yang berbeza. Kedudukan pengganti mempengaruhi ciri-ciri NLO dan optoelektronik bagi kesemua sebatian menunjukkan potensi yang menjanjikan untuk mereka bentuk bahan NLO yang maju.

**STRUCTURE CHARACTERIZATION AND NONLINEAR OPTICAL PROPERTIES OF NOVEL CHALCONE DERIVATIVES: EXPERIMENTAL AND COMPUTATIONAL INVESTIGATIONS**

## ABSTRACT

Eight fluoro methoxyphenyl chalcones derivatives (**1**-**8**) with varying substitution groups were synthesized by the Claisen-Schmidt condensation method and crystallized using slow evaporation techniques. The compounds were characterized using FTIR and NMR, as well as the 3D structural determination by SCXRD. Hirshfeld surface analysis revealed that crystal packing and molecular conformation were stabilized through hydrogen bonding, π–π stacking, and halogen interactions. The molecular properties were determined using MEP and NPA analyses. The linear and 3rd-order nonlinear optical properties were studied theoretically (using DFT and TDDFT) and experimentally (using UV-Vis spectrometer and Z-scan technique). The theoretical studies indicate that the absorption peak of compounds **1**–**8** is mainly contributed by an electronic transition from the ground state to the second excited state ($S_0 \rightarrow S_2$), with an excitation energy ranging from 4.17 to 4.29 eV, and transition electric dipole moment of 2.763 to 2.885 a.u. The experimental studies determined the two-photon absorption (2PA) of all compounds is mainly attributed to their nonlinear absorption (NLA) in the non-resonant laser regime, consistent with the trend of dynamic $\gamma_{\mathrm{DFT}}(-\omega;\omega,\omega,-\omega)$ computed using CAM-B3LYP functional at 637 nm. Furthermore, the descriptor for the metric of charge transfers molecular excitations, $\Delta$r, correlates well with the nonlinear absorption $\alpha_2$ obtained *via* open-aperture Z-scan experiment, and second order hyperpolarizabilities calculated using DFT. Nonlinear refraction (NLR) observed *via* closed-aperture Z-scan showed

negative NLR due to the self-defocusing behaviour of all compounds. The trend of $n_2$ for all compounds are exactly same with the trend of experimental $\gamma_{\exp}(-\omega;\omega,\omega,-\omega)$, indicating that NLR may be directly influenced by the different thermal diffusivity of compounds substituted with varying substituents. The position of substitution affects the NLO and optoelectronic properties of all compounds, demonstrating promising potential for designing advanced NLO materials.

# CHAPTER 1

# INTRODUCTION

## 1.1 Research Background

Nonlinear optics is a well-established and dynamic branch of photonics, that allows researchers to engineer innovative devices with great potential in various optical applications such as lasers, sensors, telecommunications, and the protection of photosensitive semiconductor devices (Boyd, 2020). However, even though scientists have made significant progress, we still encounter numerous challenges such as determining the best molecular design strategy to create great nonlinear optical materials that meet all the desired criteria. While there are currently various commercial nonlinear optical materials available, researchers are continuously searching for and working on the NLO materials that shows exceptional optical nonlinearity and high thermal resistance and are cost-effective and able to be prepared *via* green synthesis.

Many inorganic NLO research interests have been diverted into organic compounds, particularly chalcones, because they can be acquired *via* environment friendly green synthesis yet readily available as natural products, have a versatile molecular design, and possess great nonlinear optical properties resulting from inter- and intramolecular charge transfer processes (D'Silva *et al.*, 2011). In addition, the nonlinear optical properties of organic chalcones can be enhanced by the push-pull setup, where strong acceptor/donor groups are attached to the two ends of the benzene rings (Muhammad *et al.,* 2016). Besides, organic chalcones have high crystallinity, which is an advantageous property for their practical use in nonlinear optics devices (Patil *et al.*, 2007).

In summary, nonlinear optics play an important role in the development of photonics devices, and researchers are continuously working on the strategy to find the better nonlinear optical materials. Organic chalcones have attracted a lot of attention because they are abundant, can be designed flexibly at the molecular level, have exceptional nonlinear optical capabilities, and can be further tuned through push-pull arrangements.

## 1.2 Research Questions

i. How to design chalcones that have better NLO responses?

ii. How do different substituents (donors and acceptors) and varying substituent position attached to the two terminal benzene rings affect the NLO responses?

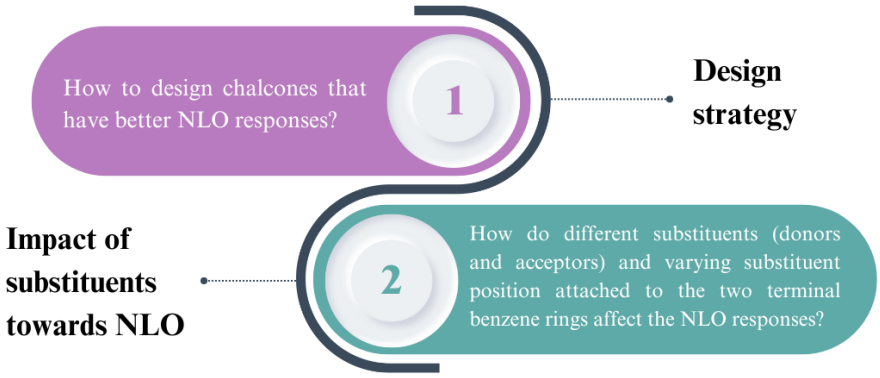


Figure 1.1 Research questions.

## 1.3 Hypothesis

i. Chalcones that have a greater push-pull setup (varying donor and acceptors) exhibit better nonlinear optical responses.

ii. The structure-property relationships for NLO materials can be investigated by combining the experimental (XRD and Z-scan) and the computational (DFT) methods.

## 1.4 Problem Statement

Currently, inorganic compounds are dominating the field of nonlinear optical materials, particularly in high-speed electro-optic modulator devices, which offer good transmission capacity for telecommunication infrastructure. However, the preparation processes for these inorganic materials are costly and it is challenging to tune the nonlinear optical responses through inorganic structural modifications. Therefore, materials scientists encounter tough challenges of producing advanced nonlinear optical (NLO) materials that are high performance and can be obtained *via* green synthesis. To address these challenges, organic NLO materials such as chalcones have emerged as promising alternatives. They have several advantages, including relatively inexpensive, environmental friendly synthesis process, high laser damage thresholds (more than 10 $GW/cm^2$ with picoseconds pulses), fast nonlinear optical response times, and possibilities to fine-tune their NLO properties through the substitution of different electron donors and acceptors (Yang *et al.,* 2020). Chalcones are chosen amongst other organic compounds because of their push-pull setup and good π-conjugation configuration which allow for a higher degree of electron delocalization, hence, enhancing the nonlinearity performance. By changing the donor and acceptor substituents and their substitution positions in the organic chalcones, allows for fine-tuning of various nonlinear optical properties such as optical limiting (OL), nonlinear refraction (NLR), nonlinear absorption (NLA), optical phase-matching, and mechanical, chemical, and thermal stabilities.

Inter- and intramolecular charge transfers (ICT) play a critical role in the first and second hyperpolarizability (β and γ) of nonlinear optical characteristics *(John et al., 2018),* respectively. Strong acceptors (A) and donors (D) located at the two terminal aromatic rings connected by a π-conjugated bridge facilitate the push-pull

configuration, enabling effective intermolecular and intramolecular charge transfers. However, the knowledge gaps pertaining to how intramolecular charge transfer contributes to the third-order nonlinear optical (NLO) responses and second hyperpolarizability have hindered its practical application in industry. Furthermore, there is a lack of understanding about the complex relationship between the structure and properties of nonlinear optical (NLO) materials, as well as the impact of donor or acceptor substituents and their positions on NLO responses. Hence, it is very challenging to develop third-order nonlinear materials that are suitable for industrial use without understanding the underlying mechanism. In this project, our aim is to investigate the relationship between the structure and NLO properties of chalcones, as well as the impact of donor or acceptor substituents on the third-order NLO responses *via* charge distribution analysis. We anticipate that this research will lead to the development of guidelines for designing highly efficient third-order NLO materials that meet the industrial needs for advanced NLO materials.

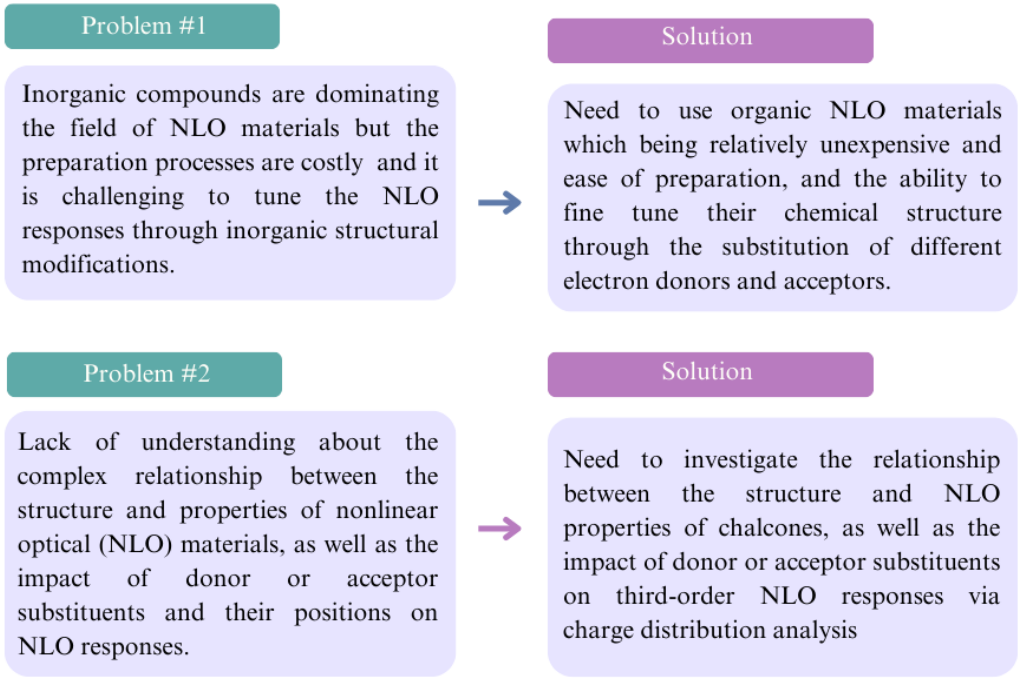


Figure 1.2 Summary of problem statement.

## 1.5 Objectives of the Research

i. To synthesize and crystallize novel chalcone compounds that exhibit good NLO responses.

ii. To investigate the effect of different substituents (donors and acceptors) and varying positions of the substituents towards NLO responses.

iii. To study the structure-NLO relationship by comparing experimental data with the density functional theory model.

# CHAPTER 2

# LITERATURE REVIEW

## 2.1 Synthesis Process of Chalcone Derivatives

Chalcone derivatives are organic compounds that consist of two aromatic rings linked by a three-carbon α, β-unsaturated carbonyl system. They are found in many plants and are the main precursors for the synthesis of a variety of other compounds such as flavonoids (Rao *et al.,* 2004), isoflavonoids, and stilbenes. They also have a wide range of biological activities, including antimicrobial (Bandgar *et al.*, 2010), anticancer (Nielsen *et al.,* 1995), antioxidant (Sivakumar *et al.,* 2007), antifungal (Svetaz *et al.,* 2004) and anti-inflammatory (Hsieh *et al.,* 2000) effects, and used as agrochemicals and have allelopathic activity (Thirunarayanan *et al.,* 2008). Chalcone synthesis can been achieved through a variety of methods as shown in Table 2.1.

Table 2.1 Methods of synthesis of chalcone.

| Method | Description | References |
|---|---|---|
| **Claisen-Schmidt Aldol Condensation** | A widely used method in chalcone synthesis, known for its environmentally friendly approach and minimal toxicity. | (Romanelli *et al.,* 2011) |
| **Suzuki Reaction** | A cross-coupling reaction used in chalcone synthesis, offering versatility in forming carbon-carbon bonds. | (Eddarir *et al.,* 2003; Selepe *et al.,* 2013) |
| **Wittig Reaction** | Involves the use of phosphorus ylides to form chalcones through olefination. | (Farooq *et al.,* 2019; Mulugeta, 2022) |
| **Friedel-Crafts Acylation** | A method that uses cinnamoyl chloride to introduce acyl groups into aromatic systems for chalcone formation. | (Nasir *et al.,* 2013; Petrov *et al.,* 2008) |
| **Photo-Fries Rearrangement** | A photochemical reaction that rearranges phenyl cinnamates to produce chalcones. | (Kawatsuki *et al.,* 2013) |

## 2.2 Push-pull System of Chalcone Derivatives

The reactions are carried out between acetophenone and benzaldehyde in the present of catalyst, as illustrated in Figure 2.1.

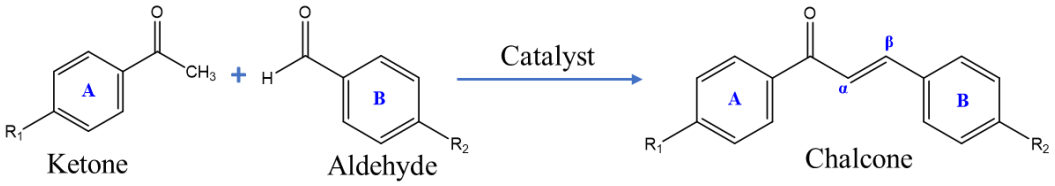


Figure 2.1 Chalcone synthesis by Claisen-Schmidt method.

Besides, chalcone derivatives are a type of organic NLO molecules that have a π-electron conjugated structure. This structure consists of an electron donor group at one terminal and an acceptor group at the opposite end. The push-pull conjugated structure (Figure 2.2) results in a notable increase in the dipole moment, which further increases the optical susceptibility of the molecule. This causes the molecule to become polarized which enhances its NLO properties (Guarin *et al.*, 2020). The π-electron conjugated system in chalcone provides a large charge transfer axis that facilitates the intramolecular charge transfer, which enhances the manifestation of NLO properties (Jia *et al.*, 2022).

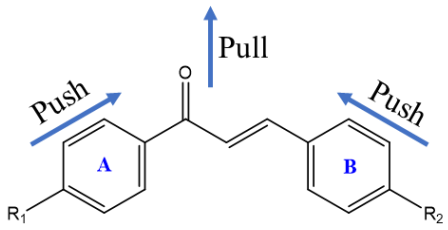


Figure 2.2 The push-pull configuration of chalcone derivative.

Furthermore, the chalcone derivatives can be easily modified by simply changing the substitution groups. The NLO properties of a molecule that corresponds to the push-pull setup can be enhanced by incorporation different electron-donating or electron-withdrawing groups (Omar *et al.*, 2020). The strength (Audebert *et al.*, 2003; Ravindra *et al.*, 2007) and position (Gandhimathi *et al.*, 2013) of substituents in the molecular structure are critical factors that affect the NLO properties of organic

compounds. The position of a substituent group can affect the degree of conjugation and resonance within the molecule, which influence the magnitude of the NLO response.

## 2.3 Nuclear Magnetic Resonance (NMR) Analysis

Nuclear magnetic resonance (NMR) spectroscopy is a method used to study the structure and composition of molecules by analyzing the magnetic properties of atomic nuclei, particularly hydrogen ($^{1}$H) and carbon ($^{13}$C) atoms. The NMR studies of chalcone derivatives primarily focus on $^{1}$H and $^{13}$C isotropic chemical shifts across a spectrum of ppm values. These shifts are influenced by the electronic environment surrounding the nuclei, as well as the nature and proximity of neighboring atoms and substituents, particularly in the enone bridge region of the chalcone structure. Several studies on $^{1}$H analyses of chalcone derivatives are summarized in Table 2.2, showing that the H$\alpha$ and H$\beta$ protons for all compounds resonated as a doublet in the region of 7.2 ppm and 7.77-8.21 ppm.

Table 2.2 $^{1}$H isotropic chemical shifts (ppm) of chalcone derivatives.

| **Literature** | **Compounds** | **$^{1}$H NMR** | | | |
|---|---|---|---|---|---|
| | | H$\alpha$ | | H$\beta$ | |
| | | Expt. | DFT | Expt. | DFT |
| (Wong *et al.*, 2022) | I | 7.56–7.52 | 7.81 | 8.21–8.17 | 8.70 |
| | II | 7.33–7.29 | 7.75 | 8.09–8.05 | 8.78 |
| | III | 7.39–7.35 | 7.83 | 8.10–8.06 | 8.60 |
| (Naik *et al.*, 2020) | 3F5B2SC | 7.37, 7.36 | 7.47 | 7.77 | 7.90 |
| | 4M5B2SC | 7.26 | 7.25 | 7.77 | 7.93 |
| (Patil *et al.*, 2019) | N-ANC | 7.46, 7.47 | 7.48 | 8.14 | 8.50 |

Wong *et al.*, (2022) reported an NMR study of chalcone, compound **III** identifying doublets corresponding to the H$\alpha$ and H$\beta$ protons of the double bond of chalcone at 7.39–7.35 ppm and 8.10–8.06 ppm, respectively (Figure 2.3). The chemical shift values reflect the interaction between the Hα and Hβ protons on the α and β carbons of the chalcone's double bond, causing them to split into doublets. These

values are typical for chalcone, influenced by its conjugated system and the electron density around the double bond. This splitting confirms the structure and behavior of the double bond in the chalcone molecule.

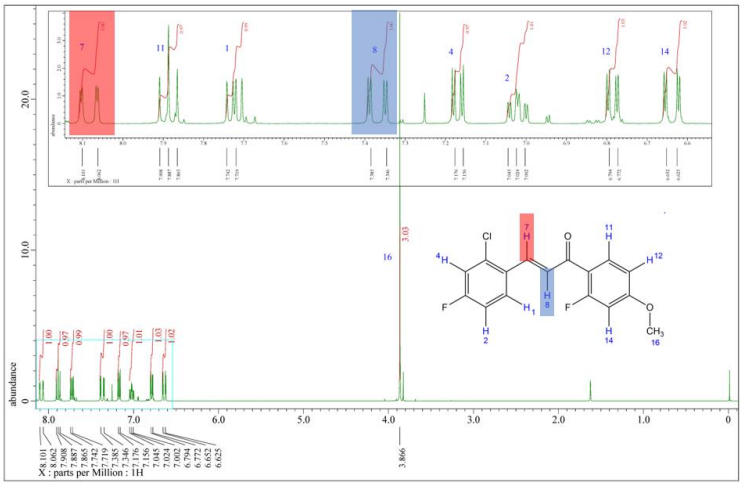

Figure 2.3 $^{1}$H NMR spectrum of compound **III** (Wong *et al.*, 2022).

Several studies on $^{13}$C NMR, focusing on C*α*, C*β* and *C = O*, are summarized in Table 2.3. In the $^{13}$C NMR spectra, the carbonyl carbon was observed in the downfield region compared to the other carbon atoms, influenced by the environment and electronegativity of the adjacent oxygen atom, which appears at around 181.96-199.26 ppm. Figure 2.4 shows the $^{13}$C NMR spectrum of compound III, as reported by Wong *et al.*, (2022).

Table 2.3 $^{13}$C isotropic chemical shifts (ppm) of chalcone derivatives.

| **Literature** | **Compounds** | **$^{13}$C NMR** | | | | | |
|---|---|---|---|---|---|---|---|
| | | C*α* | | C*β* | | C = O | |
| | | Expt. | DFT | Expt. | DFT | Expt. | DFT |
| (Wong *et al.*, 2022) | I | 122.85 | 123.41 | 139.40 | 145.46 | 192.68 | 195.23 |
| | II | 125.78 | 127.73 | 140.01 | 147.73 | 183.49 | 186.76 |
| | III | 127.81, 127.75 | 129.95 | 138.44 | 145.72 | 186.68, 186.64 | 188.59 |
| (Naik *et al.*, 2020) | 3F5B2SC | 121.76 | 120.02 | 146.91 | 147.4 | 181.96 | 180.66 |
| | 4M5B2SC | 114.55 | 115.71 | 147.45 | 148.19 | 182.48 | 180.80 |
| (Patil *et al.*, 2019) | N-ANC | 124.92 | 127.58 | 143.8 | 151.57 | 199.26 | 214.82 |

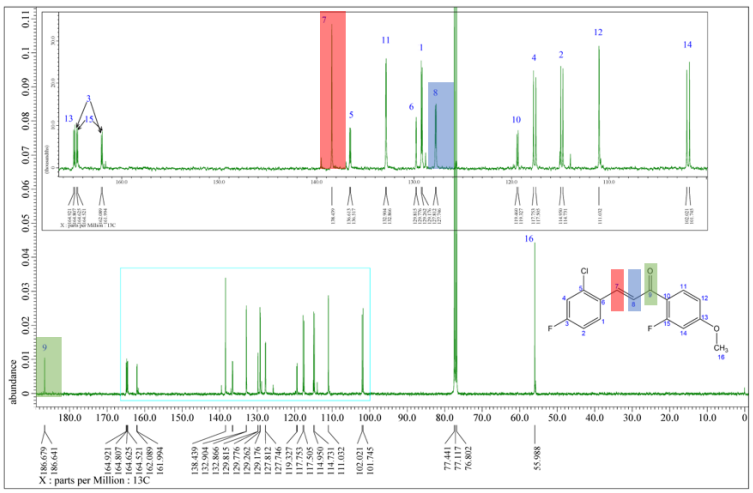

Figure 2.4 13C NMR spectrum of compound **III** (Wong *et al.*, 2022).

## 2.4 Fourier Transform Infrared (FTIR) Spectroscopy Analysis

Fourier transform infrared spectroscopy (FTIR) is a powerful technique for identifying functional groups in various materials, including gases, liquids, and solids. Attenuated Total Reflection (ATR) has become widely used in FTIR analysis due to its convenience and efficiency compared to the traditional potassium bromide (KBr) pellet method. ATR-FTIR requires minimal sample preparation, making it a preferred choice for researchers. Spectra are typically recorded in the 600-4000 $cm^{-1}$ range, allowing for easy analysis of organic compounds like chalcone derivatives (Tahir *et al.*, 2017)

In contrast, the traditional KBr pellet method involves pressing the sample into a pellet to obtain spectra in the 400-4000 $cm^{-1}$ range, which can be time-consuming and labor-intensive. Bukowski *et al.*, (2007) noted that ATR-FTIR provides a quicker and simpler alternative, eliminating the need for complex preparations and enabling more efficient quantitative analysis.

For chalcone derivatives, ATR-FTIR focuses on key vibrational modes such as phenyl ring (C═C), carbonyl (C═O), vinyl (C—H) and halogens groups (C—X, where X=F, Cl, Br) where the vibrations of these functional groups are predominated in the

spectral region. These vibrational frequencies offer important insights into the structure of chalcones, with previously reported frequencies summarized in Table 2.4.

Table 2.4 Assignment of vibrational frequencies of chalcone derivatives

| Stretching (ν) vibrational mode | Expt. ($cm^{-1}$) | DFT ($cm^{-1}$) | Literature |
|---|---|---|---|
| **νC=C** | 1636 –1590<br>1617 – 989<br>1623 – 1523<br>1576 – 1572 | 1657 – 1597<br>1595 – 982<br>1643 – 1504<br>1600 – 1570 | (Wong *et al.*, 2022)<br>(Naik *et al.*, 2020)<br>(Kumar *et al.*, 2015)<br>(Kumar *et al.*, 2015) |
| **νC=O** | 1654 – 1574<br>1650 – 1644<br>1820 – 1670<br>1656 – 1638 | 1685 – 1581<br>1649 – 1641<br>1768 – 1600<br>1715 – 1600 | (Wong *et al.*, 2022)<br>(Naik *et al.*, 2020)<br>(Kumar *et al.*, 2015)<br>(Kumar *et al.*, 2015) |
| **νC—H** | 3087 – 3048<br>3084 – 3057<br>3100 – 3000<br>3120 – 3000 | 3090 – 3078<br>3105 – 3043<br>3196 – 3166<br>3102 – 3077 | (Wong *et al.*, 2022)<br>(Naik *et al.*, 2020)<br>(Kumar *et al.*, 2015)<br>(Kumar *et al.*, 2015) |
| **νC=F/Cl/Br** | 1236 – 910<br>1221 – 505<br>505 – 503 | 1234 – 1095<br>1221 – 507<br>516 – 505 | (Wong *et al.*, 2022)<br>(Naik *et al.*, 2020)<br>(Kumar *et al.*, 2015) |

The C=C stretching vibration in chalcones typically appears in the 1636 – 1572 $cm^{-1}$ range. This is lower than the stretching frequency of isolated C=C bonds due to conjugation with the carbonyl group, which delocalizes electron density and reduces the vibrational frequency. Electron-donating or withdrawing substituents on the aromatic ring can further influence this frequency, as reported by Wong *et al.* (2022) and Kumar *et al.* (2015).

Similarly, the C=O stretching mode appears within 1820 – 1650 $cm^{-1}$, influenced by the conjugation between the carbonyl group and the C=C bond. This conjugation weakens the C=O bond slightly, resulting in lower vibrational frequencies compared to unconjugated carbonyls. The experimental data, corroborated by DFT calculations, as presented by Naik *et al.* (2020) and Kumar *et al.* (2015), show good agreement within this range.

The C–H stretching vibrations in chalcones, especially those associated with aromatic systems, are observed in the 3120 – 3000 $cm^{-1}$ range, with calculated DFT values closely aligning with experimental results. This vibrational mode is typical for $sp^2$ hybridized C–H bonds in aromatic systems, where the electron density around the carbon atoms affects the frequency, as shown in studies by Wong *et al.* (2022) and Kumar *et al.* (2015).

For halogen-substituted chalcones, the C–F, C–Cl, and C–Br stretching modes are identified between 1236 – 503 $cm^{-1}$. These frequencies are largely determined by the mass of the halogen, with heavier halogens like bromine exhibiting lower stretching frequencies, while lighter halogens like fluorine show higher frequencies, as detailed by Naik *et al.* (2020) and Kumar *et al.* (2015). Figure 2.5 illustrate FTIR spectrum of 3F5B2SC compound (Naik *et al.*, 2020).

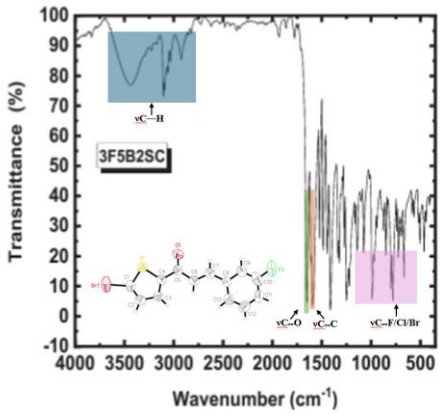


Figure 2.5 FTIR spectrum of 3F5B2SC compound (Naik *et al.*, 2020).

## 2.5 Ultraviolet-Visible (UV-Vis) Spectroscopy

UV-Vis spectroscopy is a quantitative technique that measures the amount of absorbed or transmitted by a sample in discrete wavelengths of the ultraviolet (UV) or visible (Vis) spectrum. When a molecule absorbs UV-visible light, electrons are excited from lower to higher energy levels (Wandelt, 2018). Analyzing the wavelength of spectrum, the band gap energy can be determined, which corresponds to the specific

energy required for an electron to transition from the valence band to the conduction band (Makuła *et al.,* 2018).

Ravindrachary *et al.,* (2005) reports that the crystal is transparent in the visible region with the absorption takes place in the UV range between 316 to 405nm (Figure 2.6). The maximum absorption at 337nm,which attributed to n–π* transition, likely due to to the excitation in the aromatic ring and C=O group. The absorption data reveals the extent of electron delocalization and the ground-state electron structure of the materials.

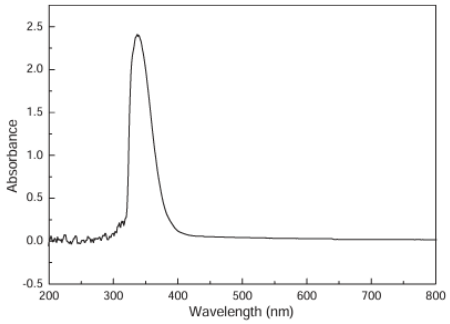


Figure 2.6 UV-Vis spectra of 1-(4-methylphenyl)-3-(4- N, N dimethyl amino phenyl)-2-propen-1-one (Ravindrachary *et al.,* 2005).

Pannipara *et al.,* (2014) investigate the impact of solvent polarity on the absorption and emission maxima in the UV-Vis investigation of the chalcone derivative 3-(1-methyl-1H-pyrrol-2-yl)-1-naphthalen-2-yl propenone (MPNP) (Figure 2.7). The wavelength shifts for the $\lambda_{max}$ values are presented in Table 2.5. MPNP exhibits a broad absorption band across various solvents, but the specific absorption maximum (λmax) shifts based on solvent polarity, revealing changes in the electronic structure of molecule as influenced by its environment. In non-polar solvents, such as hexane, the absorption maximum ($\lambda_{max}$) for MPNP is observed around 389 nm; however, in polar solvents like dimethylformamide (DMF), the absorption band shifts to approximately 395 nm. Out of all the solvents tested, DMF shows the highest

absorption wavelength maximum for MPNP, suggesting that its polarity fosters enhanced electron delocalization within the molecule. This shift in $\lambda_{max}$ across solvents highlights the sensitivity of $\pi \rightarrow \pi^*$ transition of MPNP to solvent polarity, with DMF emerging as the optimal solvent for maximizing absorption wavelength in this study. Consequently, DMF stands out as the preferred solvent for achieving peak UV-Vis absorbance in chalcone derivatives, particularly for applications where maximizing absorption is essential.

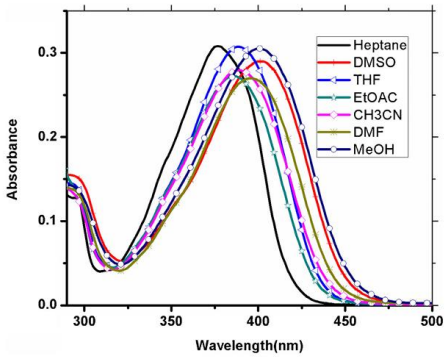


Figure 2.7 UV-Vis spectra of compound MPNP in different solvents (Pannipara *et al.*, 2014).

Table 2.5 UV-Vis absorption maximum of compound MPNP in different solvents (Pannipara *et al.*, 2014).

| Solvents | λabs(nm) |
|---|---|
| **Heptane** | 385 |
| **DMSO** | 402 |
| **THF** | 388 |
| **EtOAC** | 386 |
| **CH3CN** | 388 |
| **DMF** | 395 |
| **MeOH** | 400 |

## 2.6 X-ray Diffraction Studies

### 2.6.1 Molecular Structure of chalcone derivative

Chalcones are versatile molecules that have the ability to adopt different configurations, including cis, trans, s-cis, and s-trans forms (Figure 2.8). The arrangement of hydrogen atoms in double bond $C_\alpha$=$C_\beta$ of chalcone can be either cis or

trans, while the s-cis or s-trans formations depend on the positioning of the C=O in relation to the vinylenic double bond ($C_\alpha$=$C_\beta$), due to the unrestricted rotation along the single bond connecting C=O and $C_\alpha$ (Aksöz*et al.*, 2011)).

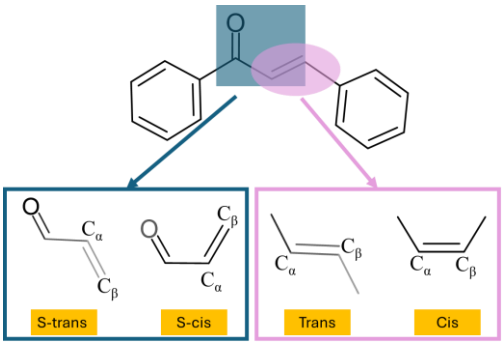


Figure 2.8 Different type of configurations (*cis, trans, s-cis,* and *s-trans*) in chalcone.

Kerek *et al.*, (2021) investigates the s-cis and s-trans conformations of 4-hydroxychalcone (Figure 2.9), focusing on their stability and electron delocalization properties. It was determined that *s-cis* conformers are more stable than s-trans conformers, primarily due to greater planarity, which enhances electron delocalization across π-orbitals. Two s-cis conformers, labeled as (a) and (b), were identified, with the s-cis (a) conformer showing the highest stabilization energy (510.37 kcal/mol) due to effective interactions between the hydroxyl group and the aromatic ring. In contrast, the s-trans conformers exhibited lower stability, attributed to a less planar structure that limits π-π interactions. This study highlights that s-cis conformations are energetically preferred due to their structural configuration, contributing to potential applications of chalcones in materials requiring stable electron delocalization.

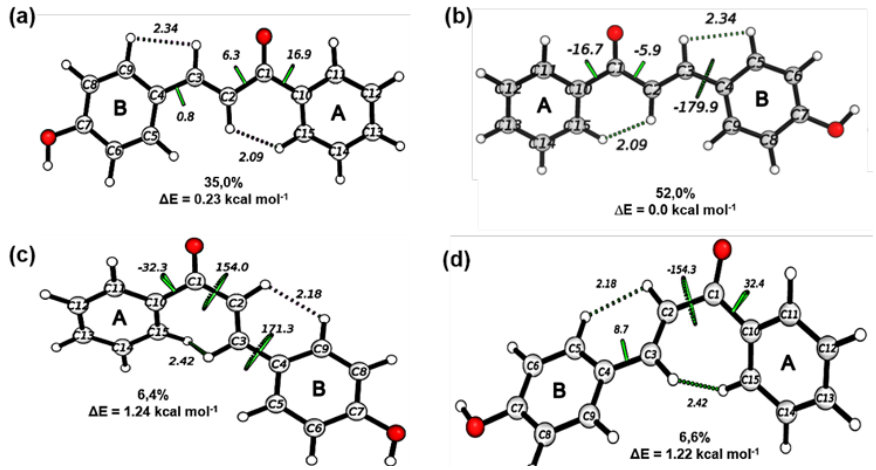


Figure 2.9 Structures of s-cis (a and b) and s-trans (c and d) conformers of 4-hydroxychalcone (Kerek *et al.*, 2021).

Naresh *et al.*, (2021) focuses on the cis and trans isomers of a chalcone derivative, specifically 1-(5-bromothiophen-2-yl)-3-(10-chloroanthracen-9-yl)prop-2-en-1-one (Figure 2.10). The synthesis and characterization of the cis and trans configurations revealed unique packing and structural characteristics. The trans isomer crystallizes in an orthorhombic system, forming a 3D zig-zag arrangement stabilized by C—H···O, C—H···Cl, and Br···π interactions. This conformation facilitates more efficient molecular packing and intermolecular connectivity. In contrast, the cis isomer crystallizes in a monoclinic structure with a 2D layered formation stabilized by C—H···O and S···S contacts. These differences highlight the role of configuration in influencing crystal packing and stability, with trans often favoring stronger packing and diverse intermolecular bonding interactions, making it more stable and structurally robust.

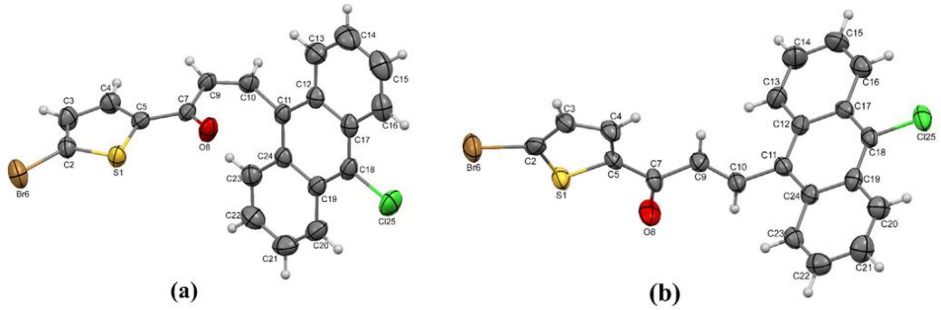


Figure 2.10 ORTEP of the (a) cis and (b) trans isomer of 1-(5-bromothiophen-2-yl)-3-(10-chloroanthracen-9-yl)prop-2-en-1-one (Naresh *et al.*, 2021).

### 2.6.2 Crystal Packing Analysis

The analysis of molecular structures and crystal packing are crucial to study the intermolecular charge transfer between the molecules. The crystal packing of the chalcone derivative, (*E*)-1-(4-bromophenyl)-3-(3-fluorophenyl)prop-2-en-1-one as reported by Zaini *et al.*, (2019), primarily features a head-to-tail arrangement. In this structure, the asymmetric unit comprises two independent molecules in s-cis configurations (Figure 2.11). Centro symmetrically related molecules form dimers through C–H···O hydrogen bonds, creating various ring motifs ($R_1^2(6)$, $R_2^2(10)$ and $R_2^2(14)$ that connect adjacent molecules. This dimerization extends into chains along the [001] axis. The Hirshfeld surface analysis highlights that H···H interactions contribute most significantly to the packing, followed by C···H and O···H interactions, suggesting that van der Waals forces stabilize the overall crystal structure in this head-to-tail formation.

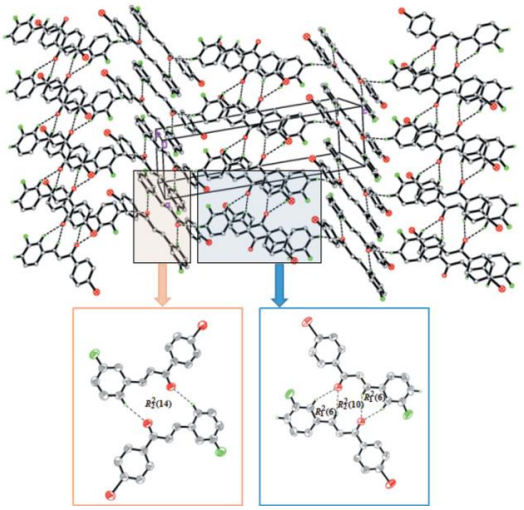

Figure 2.11 Crystal packing of the chalcone derivative, (E)-1-(4-bromophenyl)-3-(3-fluorophenyl)prop-2-en-1-one (Zaini *et al.*, 2019).

The crystal packing of two dichloro-substituted anthracenyl chalcone isomers reported by Zainuri *et al.*, (2018) is primarily organized in side-by-side arrangements. Compound I (Figure 2.12a) adopts an orthorhombic crystal structure, where the donor anthracene ring and acceptor chlorinated phenyl ring are aligned side by side, enhancing nonlinear optical (NLO) properties due to efficient molecular stacking and charge transfer interactions. In contrast, Compound II (Figure 2.12b) forms a monoclinic structure with C-H···π interactions between the anthracene ring and the phenyl group, connecting molecules into columns along the c-axis. This arrangement contrasts with the side-by-side configuration of Compound I, which shows superior NLO responses due to its optimal molecular alignment for photonic applications.

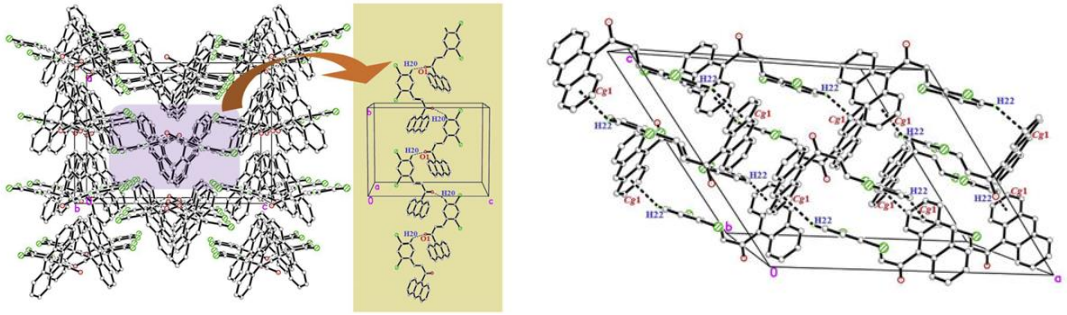

(a) (b)

Figure 2.12 Crystal packing of compounds (a) I and (b) II (Zainuri *et al.*, 2018).

## 2.7 Density Functional Theory (DFT)

Density-functional theory (DFT) is a quantum mechanical method for calculating the electronic structure of atoms and molecules, centered on electron density rather than the conventional wavefunction approach (Lewars *et al.*, 2016). As an ab initio technique, it primarily depends on atomic numbers, though some empirical parameters may be added for refinement. DFT uses electron density as a function of three spatial variables (x, y, z) in contrast to the Schrödinger equation, which depends on additional variables and thus becomes complex to solve for multi-electron systems. By using electron density, DFT offers a practical alternative for computationally complex quantum systems.

Hohenberg & Kohn, (1964) laid the theoretical foundation for DFT with two pivotal theorems. The first theorem indicates that a system's ground-state energy is uniquely defined by its electron density, making it theoretically possible to derive all system properties from electron density alone. However, this theorem does not offer a direct method for calculating the ground-state energy. The second theorem addresses this by introducing an energy functional that the ground-state electron density minimizes. This energy functional combines a universal functional which includes kinetic and electron-electron interaction energies with an external potential arising from atomic nuclei (Hohenberg & Kohn, 1964). Known as the variational principle for DFT, this approach allows the ground-state electron density to minimize the total energy functional, encompassing kinetic, potential, and exchange-correlation energies.

Kohn & Sham, (1965) further simplified DFT by proposing the Kohn-Sham equations, which model non-interacting electrons that replicate the actual system's electron density. Hohenberg and Kohn laid the groundwork for DFT in 1964 with two fundamental theorems. The first theorem posits that a system's ground-state energy is

uniquely determined by its electron density, enabling, in principle, the derivation of all system properties from this density alone. Nevertheless, there is no direct way to compute ground-state energy using this theorem. This is addressed by the subsequent Kohn-Sham method, which introduces useful equations that simplify computations and allow for accurate and efficient modelling of multi-electron systems. This technique is now a fundamental part of DFT applications, establishing DFT as a crucial computational study tool, especially in situations where conventional quantum methods would not be feasible.

### 2.7.1 Basic Sets

Basis set is a set of functions which are combined in linear combination of functions to describe the atomic molecular orbital of a molecule. The accuracy of the results is impacted by the basis set selection, which makes it significant. A larger basis set will generally provide more accurate results, but it will also require more computational resources (Magalhaes, 2014). One major limitation of DFT is slow convergence of the Kohn-Sham wavefunction for many-body systems because the small size of the one-electron basis set used to solve the equation makes it difficult to describe the short-range electron correlation around the electron-electron cusp.

Two types of functions that commonly used in basic sets are Slater-type orbitals (STOs) and Gaussian Type Orbitals (GTOs). As reported by Magalhaes, (2014), STOs describe the long-range behavior of atoms and are good at capturing charge and spin details, but they are not smooth, making them hard to use in numerical calculations. The main difference between STOs and GTOs lies in how their functions behave near the nucleus.

As described by Ulusoy *et al.*, (2019), the STOs have a cusp at the nucleus, which is important for accurately representing the strong attractive potential of the

nucleus. However, they are not smooth functions, which can make them difficult to use in numerical calculations. In contrast, Gaussian functions are smooth functions, which makes them easier to use in numerical calculations. However, they do not have a cusp at the nucleus, which can lead to errors in the calculation of the electronic wavefunction. Figure 2.13 shows the Slater function has a cusp at the nucleus, while the Gaussian function does not. In practice, Gaussian functions are preferred over Slater functions because they are more efficient in computation of the molecular integrals (simpler formulas).

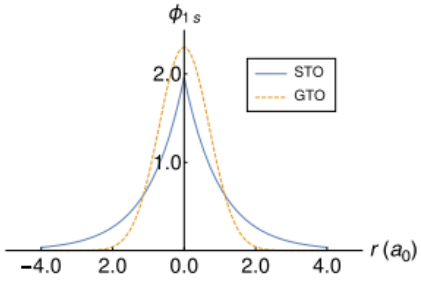


Figure 2.13 Comparison of Slater functions (STO) and Gaussian Function (GTO) (Ulusoy *et al.*, 2019)

### 2.7.2 HOMO-LUMO Analysis

The frontier orbitals in every molecule are the highest occupied molecular orbital (HOMO) and the lowest unoccupied molecular orbital (LUMO). They play a key role in determining the reactivity of the molecule. The electron from HOMO can be excited to LUMO as illustrated in Figure 2.14. The difference in energy between the HOMO and the LUMO is called the HOMO-LUMO gap (Bouzzine *et al.,* 2015). The HOMO-LUMO gap is an important property of a molecule that affects its chemical reactivity, electrical conductivity, and optical properties. A larger HOMO-LUMO gap corresponds to lower reactivity, as more energy is required to excite electrons from the HOMO to the LUMO (Maidur *et al.*, 2017).

In conjugated systems, electrons are delocalized over multiple atoms, reducing the HOMO-LUMO gap. This delocalization increases the reactivity of these molecules, as the electrons are more readily available for chemical reactions (Bouzzine *et al.*, 2015) Consequently, the smaller HOMO-LUMO gap means less energy is required for electron excitation, enhancing the optical and electrical properties of conjugated systems like chalcones.

The smaller HOMO-LUMO gap observed in these systems means that less energy is required to excite electrons from the HOMO to the LUMO, enhancing their optical and electrical properties. A smaller HOMO-LUMO gap in conjugated systems also increases their polarizability, meaning they can be easily distorted by external electric fields. This characteristic makes them excellent candidates for nonlinear optical (NLO) applications, which are crucial in technologies such as lasers, optical switches, and sensors (Steed *et al.*, 2022).

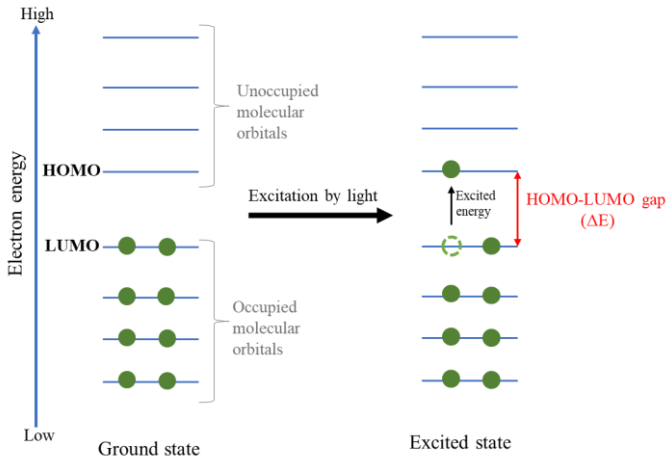


Figure 2.14 The excitation of electron passing through HOMO-LUMO gap.

Several studies have demonstrated the importance of the HOMO-LUMO gap in NLO materials. Rajan *et al.*, (2019) demonstrated a strong correlation between small HOMO-LUMO gaps and enhanced nonlinear optical responses. Their research identified molecules with delocalized π-electrons as ideal candidates for second

harmonic generation (SHG) and other NLO phenomena. Similarly, Nehru *et al.*, (2024) explored how electron-donating and electron-withdrawing groups influence the HOMO-LUMO gap and the resulting NLO properties of chalcones. Introducing strong donor groups into the molecular framework further reduces the gap, enhancing the molecule's responsiveness to external electric fields, and improving its potential for NLO applications. Figure 2.15 illustrate HOMO- LUMO plots of MMP compound (Nehru *et al.*, 2024).

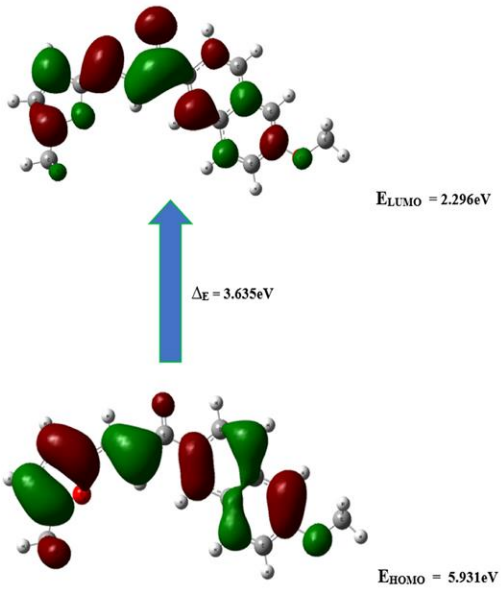


Figure 2.15 HOMO- LUMO plots of MMP compound (Nehru *et al.*, 2024).

### 2.7.3 Molecular Electrostatic Potential

The molecular electrostatic potential (MEP), which is closely related to electronic density, is an invaluable tool for understanding molecular reactivity (Priya *et al.*, 2019). By mapping MEP onto the electron density surface, one can visually identify areas prone to electrophilic and nucleophilic interactions, using distinct color codes (Zaini *et al.*, 2019).

In Figure 2.16, the study by Naik *et al.*, (2020) presents the MEP analysis of two bromo-thiophene chalcones, each containing either a fluorophenyl or

methoxyphenyl substituent. According to the authors, 3D MEP mapping reveals crucial aspects such as molecular size, shape, charge distribution, and molecular interactions. Both chalcone derivatives display a red-colored region indicating negative electrostatic potential localized around the carbonyl group, underscoring its strong electron-withdrawing capability. In compound (a), a similar red hue can be observed on the fluorine atom, consistent with its weak electron-accepting nature. Furthermore, positive electrostatic potential appears as blue regions, particularly around the protons in both compounds. Although the methoxy group in compound (b) functions as an electron-donating site (blue region), a subtle red coloration remains at the oxygen atom due to its higher electronegativity (Carvalho *et al.,* 2017).

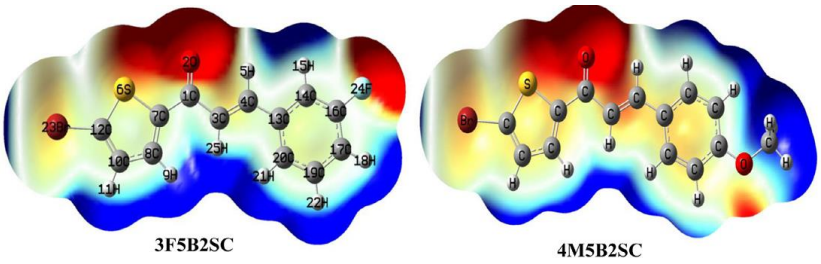


Figure 2.16 MEP plots of compounds (a) 3F5B2SC and (b) 4M5B2SC (Naik *et al.*, 2020).

Wong *et al.,* (2022) highlight the role of electrostatic potential (ESP) in understanding intermolecular interactions, using ESP maps on the molecular van der Waals (v*dW*) surface to identify reactive sites. Their analysis shows that polar surface areas for two compounds, 3A25D2 and 3A25D4 (Figure 2.17), reveal increased polarity with para- over ortho-chlorine positioning. Negative ESP regions are found around the side of the chlorine, with a small positive ESP "σ-hole" at the tip, enabling linear interactions with other molecules. The enone group further enhances interaction potential with significant negative ESP values, especially at the carbonyl oxygen, which favors interactions with chlorine in the crystal structure. Additionally, positive